Nano Energy 70 (2020) 104552

Contents lists available at ScienceDirect

Nano Energy

journal homepage: http://www.elsevier.com/locate/nanoen

Full paper

Electrolyte-assisted dissolution-recrystallization mechanism towards high energy density and power density CF cathodes in potassium cell

Cheng Jiang [a,b,1], Bojun Wang [a,1], Zhenrui Wu [a], Jiliang Qiu [c], Zhengping Ding [d], Jian Zou [a], Shulin Chen [d], Peng Gao [d], Xiaobin Niu [a,**], Liping Wang [a,b,***], Hong Li [b,c,*]

[a] School of Materials and Energy, University of Electronic Science and Technology of China, Chengdu, 611731, China
[b] Tianmu Lake Institute of Advanced Energy Storage Technologies, Changzhou, 213300, China
[c] Key Laboratory for Renewable Energy, Institute of Physics, Chinese Academy of Sciences, Beijing, 100190, China
[d] Electron Microscopy Laboratory, School of Physics, Peking University, Beijing, 100871, China

ARTICLE INFO

Keywords:
Fluorinated carbon
Fluorinated graphite
Potassium-ion battery
Concentrated electrolyte
Conversion reaction

ABSTRACT

Fluorinated carbons are reported to have the highest energy density as Li primary cell cathodes. While it has poor rate performance and the electrochemical reaction mechanism is still unclear. In this work, fluorinated graphite $CF_{0.88}$ as K cell cathode is studied. It demonstrates a better rate performance, higher operational voltage, and higher energy density than that of Li cell. Without modification, the micro-size fluorinated graphite demonstrates a specific energy density of 805 Wh kg^{-1} at 2C (1C corresponding to 821 mA g^{-1}) in K cell vs. 776 Wh kg^{-1} in Li cell. A dissolution-recrystallization mechanism is proposed for CF cathodes for discharge process. A high K ion diffusion coefficient and an early KF nucleation ascribe to its good performance. After discharge, amorphous $CF_{0.88}$ transforms to ordered graphite and KF crystals. KF particles nuclear and grow on the electrode surface. Electrolyte plays not only a role as K^+ conductor, but also a solution medium to dissolve-aggregate KF. Moreover, electrolyte salt concentration determines particle size of discharge product KF.

1. Introduction

Pursuit of batteries with high energy density and power density is always the leading goal [1,2]. Fluorinated carbons CF_x (x≈0.13–1.5), commercialized by Matsushita Electric Co. (Japan), are reported to exhibit the highest energy density in Li primary cell [3,4]. Its operational voltage depends on the carbon species, F content, and F sites [5–10]. Fluorinated graphite $CF_{1.0}$ provides a theoretical specific capacity of 865 mAh g^{-1} and an experimental operational voltage at ~3.0 V vs. Li^+/Li, providing an energy density of about 2600 Wh kg^{-1} [11]. This is much higher than other Li primary cells, such as Li/$SOCl_2$, Li/SO_2, Li/CuO, Li/CuS, Li/MnO_2, and Li/CuO. Thus, Li/CF_x cells have wide applications in commercial, industrial, medical, and military markets.

The main challenge for CF cathodes is their poor rate performance. Generally, poor rate performance is ascribed to their low electronic conductivity with insulator nature. Various strategies are employed to enhance the rate performance, such as reducing its particle size via ball-milling [11], adding conductive material polypyrrole [12], producing F-graphene layers as shell [13] and fabricating hybrid materials MnO_2/CF_x [14]. Actually, it is reported that the rate-determine step in carbon fluoride is charge-transfer rate by Lewandowski and co-authors [15].

Meanwhile, its reaction mechanism remains elusive. In the solid-state electrolyte system, it is reported that it undergoes a conversion reaction mechanism, namely, $CF_x + xLi^+ + e^- \rightarrow C + xLiF$, where both carbon and LiF are amorphous [16]. Nevertheless, in the liquid electrolyte system with the presence of solvents, it forms well-crystalline LiF and amorphous carbon. Meanwhile, the LiF particle sizes vary from nanosize to microsize in different electrolytes and temperatures, which hints that the electrolytes take part in the reaction. Read et al. obtained LiF with 30 nm at −20 °C and 60 nm at 70 °C [17] in 1 M $LiBF_4$/PC-DME electrolyte. Lewandowski et al. obtained LiF crystals with 5–20 μm in $LiPF_6$ PC-DMC+10 wt% VC electrolytes [15]. The particles are deposited

* Corresponding author. Institute of Physics, Chinese Academy of Sciences, Beijing, 100190, China.
** Corresponding author.
*** Corresponding author. School of Materials and Energy, University of Electronic Science and Technology of China, Chengdu, 611731, China.
E-mail addresses: xbniu@uestc.edu.cn (X. Niu), lipingwang@uestc.edu.cn (L. Wang), hli@iphy.ac.cn (H. Li).
[1] These authors contributed equally to this work.

https://doi.org/10.1016/j.nanoen.2020.104552
Received 12 December 2019; Received in revised form 20 January 2020; Accepted 29 January 2020
Available online 31 January 2020

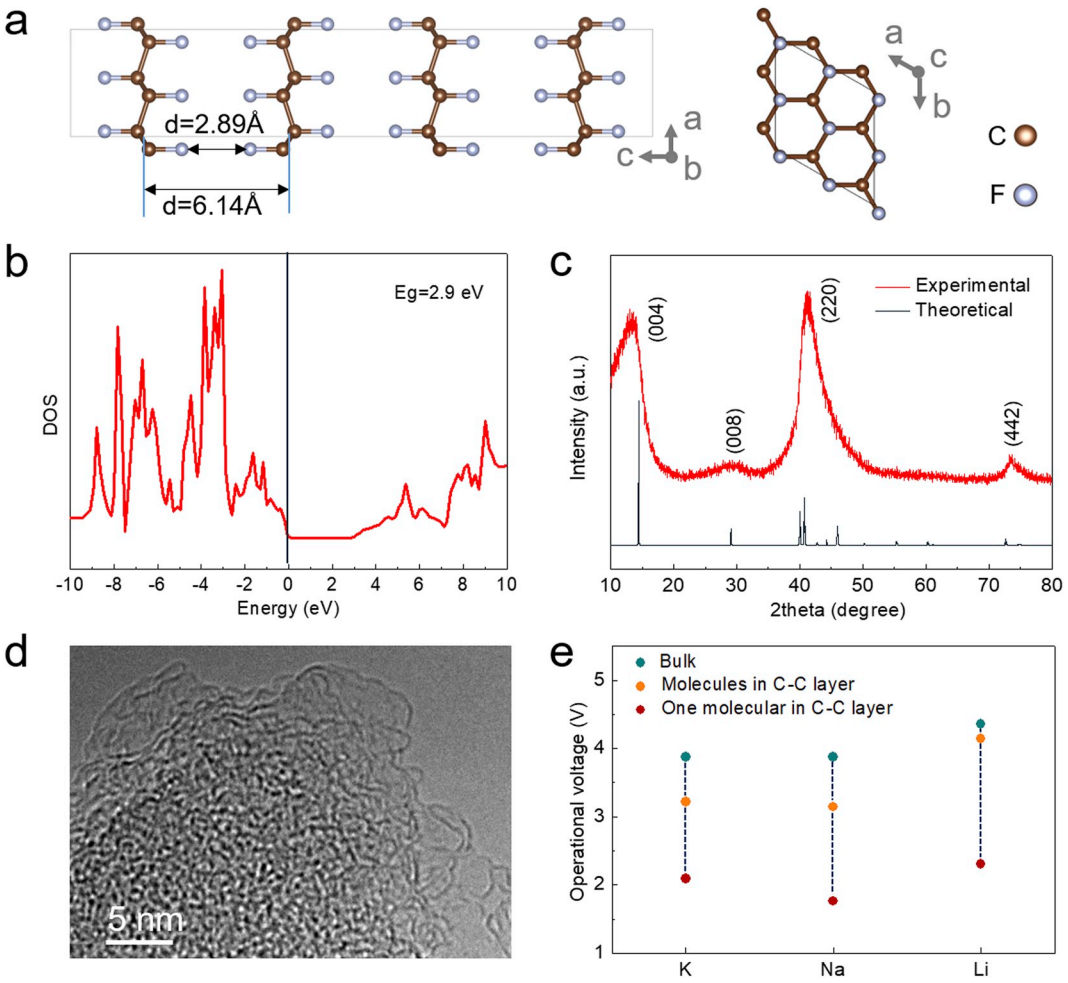

Fig. 1. (a) Crystallography of fluorinated graphite. (b) Density of states (DOS) of fluorinated graphite by first-principle calculations. (c) XRD pattern of fluorinated graphite. (d) TEM image of fluorinated graphite with amorphous state. (e) Theoretical operational voltages for fluorinated graphite cathode in K cell, Na cell, and Li cell.

on the electrode surface, demonstrating that the F^- ions can diffuse in the electrolyte. Moreover, the anions (i.e., PF_6^-, BF_4^-, ClO_4^-) are suspected to play a role in their operational voltage and capacity [18]. Note that kinetics correlated with the ionic conductivity of electrolyte cannot fully explain this phenomenon as a high operational voltage should have a high specific capacity. In words, electrolytes including salt and solvents impact its thermodynamic and kinetic behaviors in the CF cathodes.

Recently, K-ion batteries raise a widespread interest [19,20]. Potassium is an abundant element on earth. It brings in possible low cost batteries. In addition, the standard potential for K^+/K is −2.97 V vs. standard hydrogen electrode (SHE), which can provide a high energy density. For example, Prussian blue $K_2Mn[Fe(CN)_6]_y$ has a higher operational voltage (3.8 V) and a higher energy density (521 Wh kg^{-1}) in K-ion battery than the analogues $Na_2Mn[Fe(CN)_6]_y$ (3.4 V, 476 Wh kg^{-1}) in Na-ion battery and $Li_2Mn[Fe(CN)_6]_y$ (3.3 V, 446 Wh kg^{-1}) in Li-ion battery [21]. Moreover, metal ions normally bind solvents in the liquid electrolyte, where K^+-solvent has a smaller stokes radius than Li^+-solvent and Na^+-solvent in various solutions [22]. Thus, K-ion batteries can possibly have high power performance.

Thus, with the aim to improve the rate performance of CF, we apply fluorinated carbons as K primary cell cathodes in this study. It demonstrates a superior rate performance than that in Li cell. We purpose a dissolution-recrystallization reaction mechanism to explain the formation of KF crystals and defect-rich graphite. The impact of electrolytes on their rate performances is systematically studied. A high concentration K^+ at the electrode-electrolyte interface is favorable for KF nucleation and growth.

2. Experimental section

2.1. Fluorinated carbons

Fluorinated graphite $CF_{0.88}$, fluorinated carbon nanotubes $CF_{0.97}$, and fluorinated graphene $CF_{0.98}$ were bought from Hubei Zhuoxi Fluorochemical Co., LTD, China, which are produced via reactions of carbon with F_2 at about 400 °C.

2.2. Theoretical calculations

The atomic and electronic structure of graphite fluoride CF were calculated using density functional theory (DFT) with Vienna Ab-initio Simulation Package (VASP) [23,24]. The electron-ion interaction was described by projector-augmented wave method (PAW) [25] while the exchange-correlation energy was estimated by the Gradient Generalized Approximation (GGA) of Perdew-Burke-Ernzerhof (PBE) [26]. The Kinect energy cut-off was fixed at 500 eV and the spin polarization was able for all calculations. For geometry optimizations and total energy calculations, the Brillouin zone was sampling by 7 × 7 × 3 K-points grids while denser 11 × 11 × 5 K-points grids were utilized for accurate electron structure calculation. All structures were fully optimized with a 10^{-6} eV threshold of self-consistent field calculations till the residual force less than 10^{-2} Ev $Å^{-1}$.

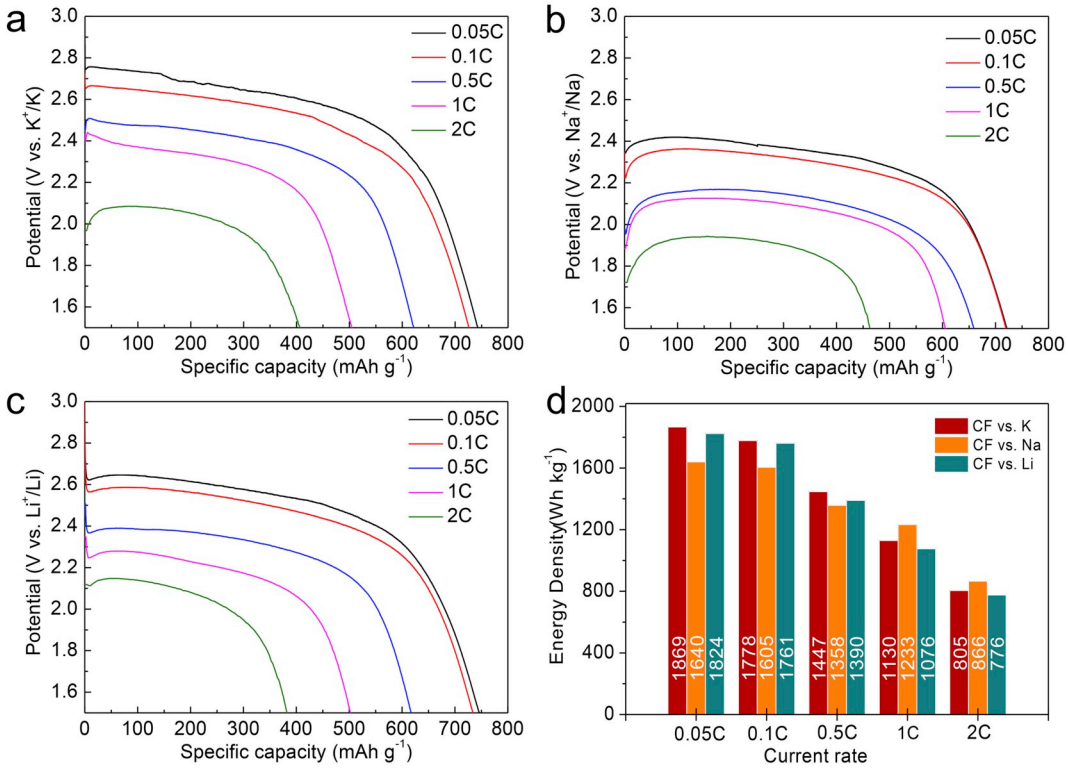

Fig. 2. Rate performances of fluorinated graphite as cathode in (a) K cell, (b) Na cell, (c) Li cell. (d) A summary of energy density as a function of current rate.

The theoretical binding energy of K^+, Na^+, and Li^+ with conventional carbonate solvents was estimated using Gaussian (G09) [27] software with Becke, 3-parameter, Lee-Yang-Parr (B3LYP) hybrid functional [28] and 6-311G++(d, p) basis. The integral equation formalism variant of the Polarizable Continuum (IEFPCM) model was applied to describe the solvation effect [29,30].

3. Results and discussion

The crystallography structure of fluorinated graphite CF is shown in Fig. 1a, consistent with the report by Touhara and coauthors [31]. Different from the pristine graphite with AB stacking layer and all the carbon atoms in the same plane, CF is a cyclohexane chair type structure with AA' stacking. Carbon atoms bond F atoms making it forming sp^3 hybrid structure instead of sp^2, like a "polymer" [32]. With the F intercalation, the C–C interlayer distance increases from 3.36 Å to 6.14 Å. This structure has a bandgap of 2.9 eV based on DFT calculations (Fig. 1b). It has an electronic conductivity of lower than 10^{-10} S cm^{-1} (out of our measurement range). Its phase is identified via XRD (Fig. 1c), which is mainly a disordered phase or hard carbon feature. It is due to the fluorine intercalation and the strong repulsion of the unshared lone pair electrons in F atoms. The amorphous structure is confirmed by TEM (Fig. 1d). The particles have micrometer size from 1 to 30 μm as shown in SEM images (Fig. S1). Based on the conversion reaction type equation $CF_{(crystalline)}+M\rightarrow MF_{(bulk)}+C_{(graphite)}$, its electromotive force (E^o) for bulk CF cathode as K, Na, and Li ion battery are 3.87 V, 3.88 V, and 4.36 V, respectively (Fig. 1e). While, given that the M (M = K, Na, Li) ions insert into carbon layer and forming C–F-M species ($CF_{(crystalline)}+M\rightarrow$C–F-M), the operational voltages may vary from that of forming bulk MF species in conventional conversion reaction. Two models via theoretical calculations are used to estimate the operational voltages of C–F-M reactions with ion inserting mechanism and the impact of F stoichiometry. In one model (called "molecules in C–C layer" model), we simulate the M ions inserting mechanism and place two layers of MF between two-layer graphene with preserved F hexagonal symmetry (Fig. S2). The "molecules in C–C layer" represents the early stage of cathode reaction with high F stoichiometry and the operational voltages are 3.22 V, 3.14 V, and 4.14 V for K cell, Na cell, and Li cell, respectively. Once the formed KF dissolves into the electrolyte, the remained CF_x have a decreased operational voltage with a decreasing F stoichiometry. To reflect the influence of F stoichiometry, we considered a F-poor limited condition with one F atom in the 5 × 5 unit cell per graphite layer for forming one molecular MF (Fig. S3) as the other model (called "one--molecular in C–C" model). The operational voltage of "one-molecular in C–C″ model is calculated to be 2.09 V for K cell, 1.76 V for Na cell, and 2.30 V for Li cell. The reported experimental results (e.g., ~3.0 V for LIBs [18] and ~2.75 V for SIBs [5]) are next to the theoretical calculations of "molecules in C–C layer" at the early stage reaction and "one-molecular in C–C″ model at the final stage reaction rather than bulk phase MF, which indicates that CF is different from traditional conversion reaction cathodes.

Fig. 2 shows the discharge performances of fluorinated graphite as KIBs, SIBs, LIBs cathode under various current density. With the increase of current density, fluorinated graphite suffers from a heavy voltage and capacity decay, leading to a fast energy density decrease. The cathode in K cell offers an energy density of 1869 Wh kg^{-1} at 0.05C, 1778 Wh kg^{-1} at 0.1C, 1447 Wh kg^{-1} at 0.5C, 1130 Wh kg^{-1} at 1C, and 805 Wh kg^{-1} at 2C. While in Li cell, it has an energy density of 1824 Wh kg^{-1} at 0.05C, 1761 Wh kg^{-1} at 0.1C, 1390 Wh kg^{-1} at 0.5C, 1076 Wh kg^{-1} at 1C, and 776 Wh kg^{-1} at 2C. In Na cell, it has an energy density of 1640 Wh kg^{-1} at 0.05C, 1605 Wh kg^{-1} at 0.1C, 1358 Wh kg^{-1} at 0.5C, 1233 Wh kg^{-1} at 1C, and 866 Wh kg^{-1} at 2C. Among them, the Na cell delivers the highest rate performance at 1C and 2C. Meanwhile, it reveals that the energy density in K cell always outperforms that in Li cell. The discharge curves of graphite fluoride in both Na cell and Li cell have an initial voltage drop followed by a voltage increase. This means that they have a big electrochemical polarization (i.e., low charge-transfer rate). On the other hand, it is noticed that the operational potential in K cell is higher than that in Na cell and in Li cell under the same current rate. It is worthy to identify whether it is a thermodynamic behavior or a kinetic behavior.

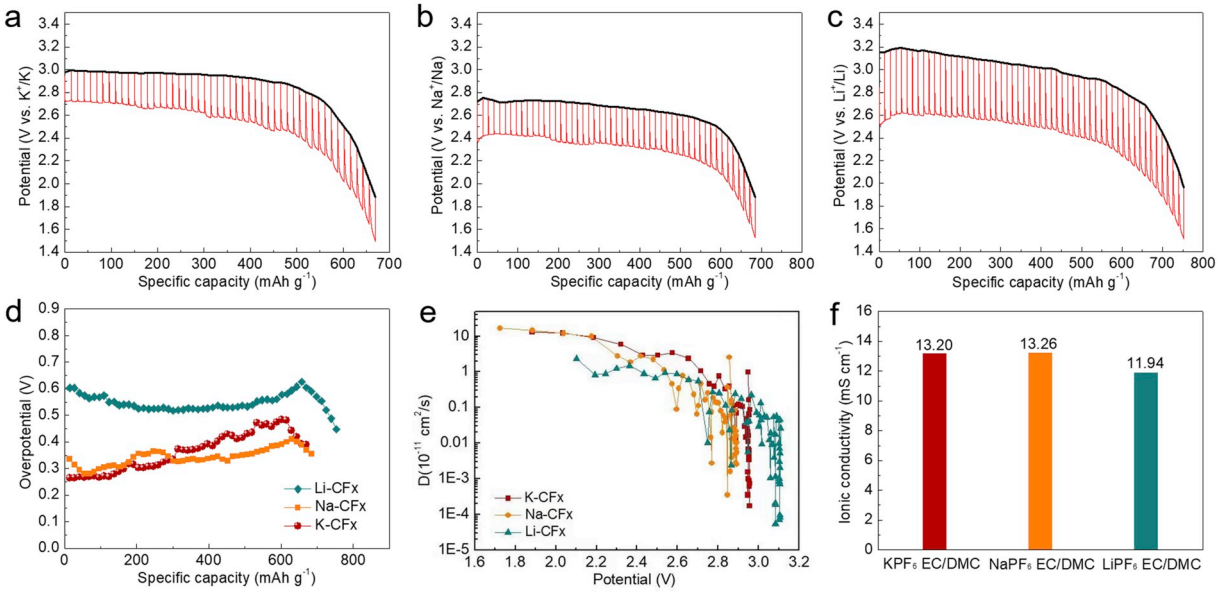

Fig. 3. GITT curves of fluorinated graphite as cathode of (a) K cell, (b) Na cell, (c) Li cell at a pulse current of 0.05C (41 mA g^{-1}) for 20 min, then a rest of 4 h. (d) Over-potential based on GITT curves. (e) Ionic diffusion coefficient calculated based on GITT curves. (f) Ionic conductivity of 1 M electrolytes MPF_6 EC/DMC (M = K, Na, Li) at room temperature.

Herein, as shown in Fig. 3a–c, GITT techniques is applied to exploit more information. Their over-potentials are correspondingly determined (Fig. 3d). After a relaxation of 4 h, their equilibrium voltage curves present a plateau shape followed by a slopy shape indicating that a phase transition first and then a solid-solution step, which fits our "molecules in C–C layer" model first and then the "one-molecular in C–C′ model. Meanwhile, their equilibrium voltages are ~3.0 V, ~2.7 V, and ~3.1 V in K, Na, and Li cell, respectively. These values are similar with the reported results [12,18,33]. The over-potential is about 0.6 V in Li cell, while it is 0.25 V in K cell. Thus, the high operational voltage embodying in K cell originates from small polarizations. The voltage hysteresis is relatively smaller than conventional conversion type cathodes, such as Fe_3O_4 (~0.7 V) and Co_3O_4 (~1.2 V) [34]. Meanwhile, the ionic diffusion coefficients are obtained based on the GITT curves, as demonstrated in Fig. 3e. The K^+ diffusion coefficient is 10^{-14} -10^{-10} cm^2 s^{-1}, which is similar with that in Na cell, but much higher than that in Li cell (10^{-15}-10^{-11} cm^2 s^{-1}). Cyclic voltammetry at different scan rates are studied (Fig. S4). The current has a linear relationship with the square root of the scan rate, which means CF is a diffusion-control step. The ionic conductivity of electrolyte is important to the kinetics. The ionic conductivities are 13.20 S cm^{-1} for 1 M KPF_6 EC/DMC, 13.26 S cm^{-1} for 1 M $NaPF_6$ EC/DMC, and 11.94 S cm^{-1} for 1 M $LiPF_6$ EC/DMC

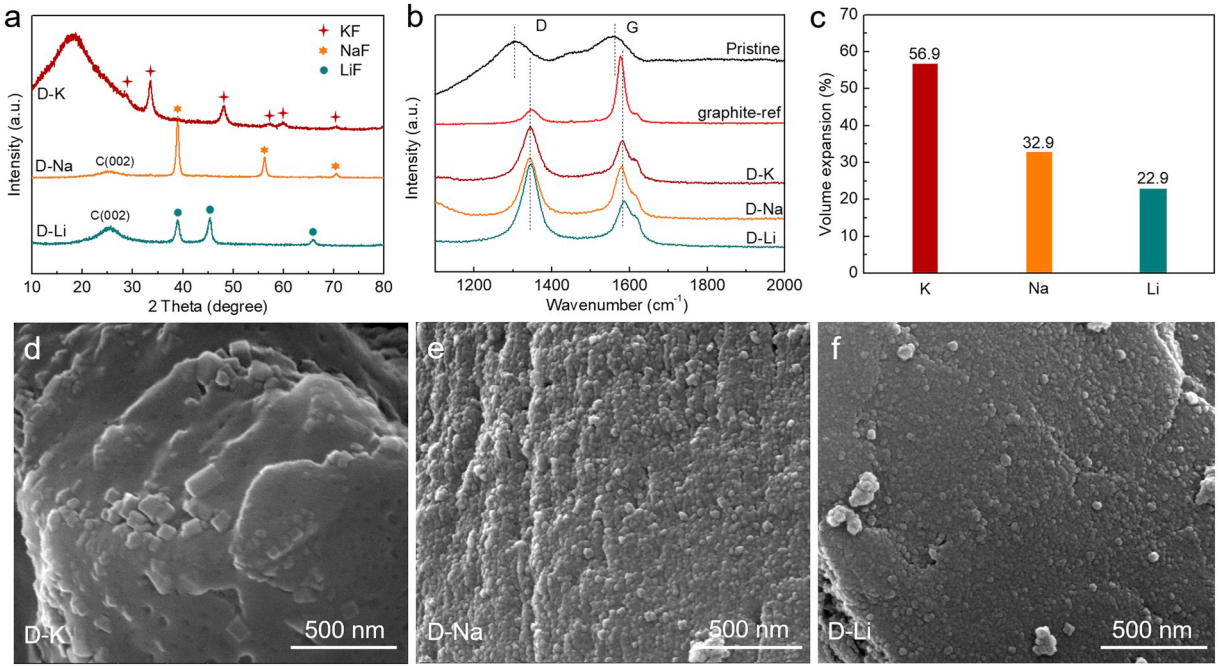

Fig. 4. (a) XRD patterns of fluorinated graphite at discharged state of 1.5 V. (b) Raman spectroscopy of fluorinated graphite at pristine and discharged state of 1.5 V. (c) Theoretical volume expansions of fluorinated graphite cathode after discharge. SEM images of fluorinated graphite at discharged state 1.5 V in (d) K cell, (e) Na cell, (f) Li cell.

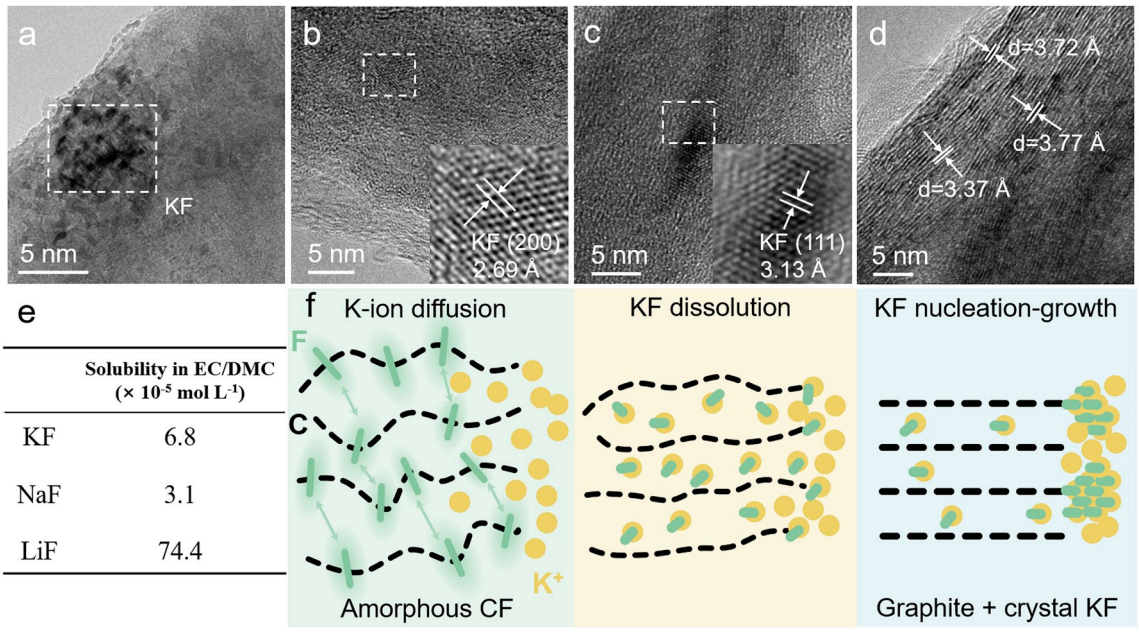

	Solubility in EC/DMC ($\times 10^{-5}$ mol L^{-1})
KF	6.8
NaF	3.1
LiF	74.4

Fig. 5. TEM images of fluorinated graphite with a discharge specific capacity of 200 mAh g^{-1} (a, b) and a discharge specific capacity of 700 mAh g^{-1} (c, d) in KPF_6 EC-DMC electrolyte. (e) Metal fluoride solubility in EC/DMC solvents. (f) A dissolution-recrystallization mechanism illustration for the fluorinated graphite reaction mechanism in the discharged process.

(Fig. 3f). Overall, EC with high-dielectric-constant has a low binding energy for a high ion mobility, while DMC with low-viscosity has a high binding energy which leads a difficulty in dissociation with the salts. Meanwhile, we calculate the binding energy between the alkaline ions (K^+, Na^+, Li^+) and carbonate solvents. The binding energy for K^+, Na^+, and Li^+ with EC is −0.14 eV, −0.15 eV, and −0.18 eV, respectively (Fig. S5). Simultaneously, the binding energy for K^+, Na^+, and Li^+ with DMC are −0.34 eV, −0.43 eV, and −0.58 eV, respectively. This is similar with the results reported by Yoon and coauthors [35]. A low bind energy leads a high ionic conductivity, which is in line with our experimental results. In words, the high power performance is a kinetic behavior rather than a thermodynamic behavior; fast K ion diffusion coefficient and the K ion electrolyte with high ionic conductivity are benefit to the high rate performance of $CF_{0.88}$ in K cell.

The discharged states for fluorinated graphite at 1.5 V are investigated via XRD (Fig. 4a). All of them form well-crystalline metal fluorides. The discharged sample in K cell is sealed by Kapten film before characterization as KF is sensitive to moisture. Thus, a broad amorphous peak of the Kapten film is observed before 2theta of 20°. The characteristic peaks for graphite (002) are also obtained, which is an exfoliated nature as the diffraction intensity is relatively weak and the diffraction peaks are broad. Raman spectroscopy is employed to detect its disordered degree (Fig. 4b). It is known that G band (~1580 cm^{-1}), an in-plane vibrational mode, provides the number information of layers and D band (~1360 cm^{-1}) originates from disordered structure. Therefore, the intensity ratio I_D/I_G is frequently used to identify the disorder degree of carbon materials. The D band and G band have a reduction in intensity and anomalous redshift in fluorinated graphite, which can be due to sp^2-sp^3 hybridization transition and formation of puckered C–C layers [36]. The I_D/I_G ratio for graphite is 0.22 in our previous study [32]. After the discharge process to 1.5 V, the I_D/I_G ratio is 1.36 for K cell, 1.10 for Na cell, and 1.91 for Li cell. The increase in the I_D/I_G ratio reveals that the obtained carbons are highly disordered. K ions with a larger radius into CF consequence a smaller disorder degree than that of Li ions insertion, which demonstrates it is not a solely insertion mechanism. Need mention that the electrodes suffer from volume expansion and partly peel off from the current collector after discharge. The theoretical volume expansions for the fluoride graphite to be $C_{(graphite)}$+ bulk MF are 56.9% in K cell, 32.9% in Na cell, and 22.9% in Li cell (Fig. 4c). The volume expansions make a worse electrical contact rendering increased electrochemical polarizations, as evidenced in the GITT results (Fig. 3d). Their discharged morphologies are measured via SEM (Fig. 4d–f). There are KF, NaF, and LiF particles on the fluorinated graphite surface, which means that F^- ions diffuse and accumulate on the surface. Different from the solid-state electrolyte system, which forms amorphous LiF in Li cell [16], the liquid environment assists KF molecules diffusion to form crystals from the carbon layer into surface, especially in K-ion liquid electrolyte.

In order to find the detailed metal fluoride formation process, we use TEM to track their morphology and structure evolution at states of 200 mAh g^{-1} and 700 mAh g^{-1} (at 1.5 V) for fluorinated graphite in K cell (Fig. 5a–d) and in Li cell (Fig. S6). Controlling the discharge capacity to be 200 mAh g^{-1}, the KF is dispersed on the surface (Fig. 5a) and in the carbon layers (Fig. 5b). The CF framework is mainly an amorphous state. After a full reaction with a capacity of 700 mAh g^{-1}, there are a few particles in carbon layers. Most of the KF particles with size of 100–300 nm are agglomerated on the surface (Fig. 4d), while we are unable to collected them as the KF on carbon surface is unstable to the electron beam of TEM (Fig. 5c and d). Surprisingly, the framework has a better crystallinity with ordered structure, like graphite. The interlayer distance is 0.33 nm–0.38 nm (Fig. 5d). Fluoride graphite after discharge process in Li cell also demonstrates a graphite structure. All of these point out that the F^- ions diffuse out of the layer. After the K ions insert into the C–C layer under the concentration gradient and electrical field force, they react with F^- to form KF at an atomic level. Once the F lose bonding with C, the C–C layer space has the ability (6.14 Å for pristine) to accommodate the electrolyte solvents. The electrolyte solvent dissolves the KF molecules. The KF concentration increases with the discharge capacity leading a critical concentration to nuclear. The solubility of KF, NaF, and LiF in EC/DMC solvent is 6.8×10^{-5} mol L^{-1}, 3.1×10^{-5} mol L^{-1}, and 7.44×10^{-4} mol L^{-1} by ICP test, respectively (Fig. 5e). Since the K^+ concentration (1 mol L^{-1}) is much higher at the electrode-electrolyte interface than that in the electrodes, the KF at the interface tends to saturate and nuclear. As a consequence, we find the electrode-electrolyte interface acts as the nucleation site and KF particles accumulate on the site for lowering surface energy. Based on these,

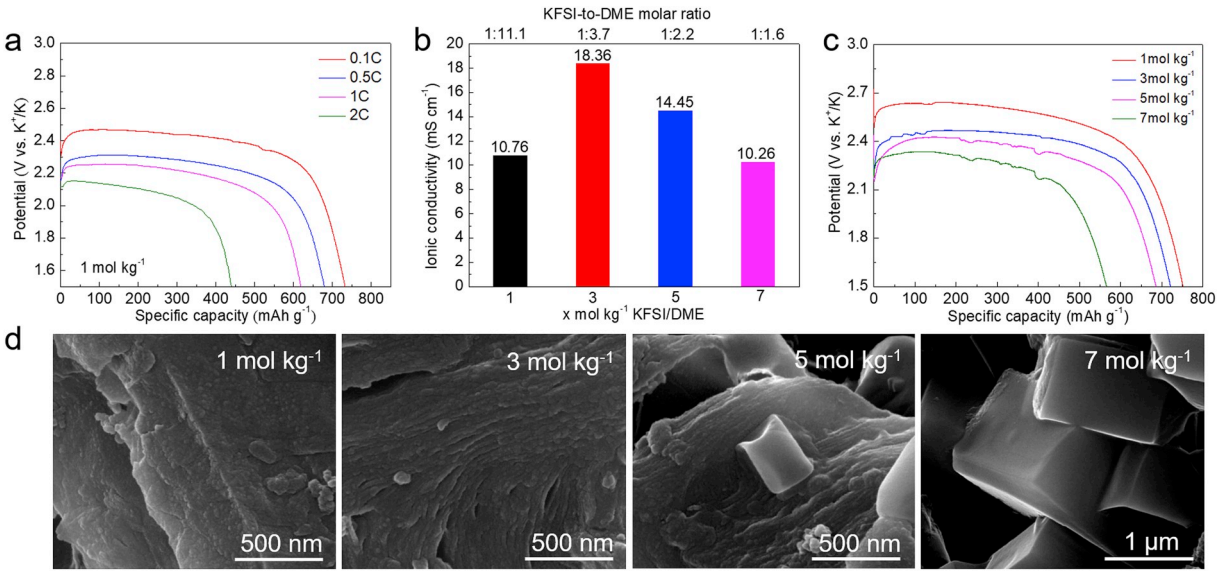

Fig. 6. (a) Rate performance of fluorinated graphite in 1 mol kg^{-1} KFSI/DME. (b) Ionic conductivity of KFSI/DME with various salt concentrations. (c) Electrochemical performance of fluorinated graphite at 0.05C in KFSI/DME with various concentrations. (d) SEM images of fluorinated graphite at the discharged state of 1.5 V in different salt concentrations of KFSI/DME.

a dissolution-recrystalline mechanism is proposed, as illustrated in Fig. 5f. It seems that a lower solubility of KF and NaF, which makes a faster nucleation than LiF under the same electrolyte concentration, is propitious to the rate performance. The as-formed KF might serve as a fulcrum in the C–C layer for a better solvent penetration. Need mention that a fast crystal growth leads an increased polarization as KF crystals block K^+ transportation (as shown in Fig. 3d at late discharged stage).

As the electrolyte takes part in the reaction, we investigate the solvent and salt effects. Ether solvents are known to have good ionic conductivity, low viscosity, and low charge-transfer resistance with the electrodes [37]. Here the DME solvent performance is studied. It is found that 1 mol kg^{-1} (namely 0.87 mol L^{-1}) KTFSI/DME electrolyte provides a similar discharge behavior with the KPF_6 EC/DMC. As shown in Fig. 6a, it demonstrates a superior rate performance with 1719 Wh kg^{-1} at 0.1C, 1497 Wh kg^{-1} at 0.5C, 1332 Wh kg^{-1} at 1C, and 903 Wh kg^{-1} at 2C. Meanwhile, the effect of salt concentration KTFSI/DME electrolytes (1 mol kg^{-1} to 7 mol kg^{-1}) is investigated. Based on the ionic conductivity equation $\sigma = \sum nqu$, where σ is the ionic conductivity, n is the carrier concentration, μ is the carrier mobility, the increase in the concentration leads a high n but a low μ due to a high viscosity [38]. Obeying this equation, their ionic conductivities are obtained to be 10.76 S cm^{-1} for 1 mol kg^{-1}, 18.36 S cm^{-1} for 3 mol kg^{-1}, 14.45 S cm^{-1} for 5 mol kg^{-1}, and 10.26 S cm^{-1} for 7 mol kg^{-1}, as shown in Fig. 6b. In contrast, with the increase of salt concentration both the specific capacity and operational voltage decrease leading a reduced energy density (Fig. 6c). At 0.05C, the energy density is 1864 Wh kg^{-1}, 1693 Wh kg^{-1}, 1573 Wh kg^{-1}, and 1251 Wh kg^{-1} in the electrolyte of 1 mol kg^{-1}, 3 mol kg^{-1}, 5 mol kg^{-1}, and 7 mol kg^{-1}, respectively. This is different from the graphite, which has a high specific capacity and high energy density in high concentrated electrolyte [39]. It is obvious that salt concentration rather than ionic conductivity is the key-determine factor for the energy density. Their morphologies after discharged to be 1.5 V are demonstrated in Fig. 6d and Fig. S7. The KF crystal sizes increase rapidly with the salt concentration, from nanosize to ~2 μm on the surface. A low concentration KF in the solution can be easily saturated in highly concentrated salt (high K^+) as the solubility product K_{sp} of KF is constant. Thus, an early nucleation and many inoculating seeds agglomeration bring in large particle sizes. As the formed KF crystals have smooth surface, it is an Ostwald-ripening growth model [40]. It is noteworthy that beyond the effects of solvent and salt concentrations, the anions (PF_6^-, $TFSI^-$) have influences on the electrochemical performance with different operational voltages (Fig. S8), but similar specific capacity. Simultaneously, the fluoride graphene and fluoride CNTs demonstrate the same behavior (Fig. S9). The anion effect demonstrates similar behavior in Li cell (Fig. S10). The ionic conductivity cannot fully interpret this as 1 M KPF_6 EC/DMC with low ionic conductivity (13.2 mS cm^{-1}) delivers higher potential than that of 1 M KTFSI EC/DMC (14.6 S cm^{-1}). It is known that the PF_6^- has a radius of 2.5 Å and $TFSI^-$ has a radius of 3.3 Å [41]. Both of them have difficulty in penetrating into the graphite electrode. It is suspected that PF_6^- dissociates into F^- and PF_5 and make the nucleation of KF more easily. A fast nucleation endows a better kinetic presenting a high operational voltage, which is a similar effect with the low solubility of KF in EC/DMC.

4. Conclusions

In summary, amorphous fluorinated graphite $CF_{0.88}$ as the K primary cell cathode is studied. Under a dissolution-recrystalline mechanism, fluorinated graphite demonstrates a higher rate performance, a higher operational voltage, and a higher energy density in K cell than that in Na cell and Li cell. In 1 mol kg^{-1} KTFSI-DME electrolyte system, fluorinated graphite $CF_{0.88}$ outputs an energy density of 1864 Wh kg^{-1} at 0.05C. A fast K ion diffusion coefficient and an easy nucleation of KF offer high energy density and power density performance. Different from the conventional conversion reaction mechanism, electrolyte provides a medium to form well-crystalline KF and graphite at the discharged state. Moreover, electrolyte-electrode interface provides a KF nucleation site; electrolyte salt concentrations are crucial to the particle size of KF. This study reveals that K-ion batteries can be promising high energy density and power density storage devices. Moreover, our study sheds light on the pivotal role of electrolyte in electrochemical performance and reaction mechanism.

Declaration of competing interest

There are no conflicts to declare.

Acknowledgments

This work is supported by the Fundamental Research Funds for the

Central Universities, China (ZYGX2019Z008).

Appendix A. Supplementary data

Supplementary data to this article can be found online at https://doi.org/10.1016/j.nanoen.2020.104552.

References

[1] L. Wang, Z. Wu, J. Zou, P. Gao, X. Niu, H. Li, L. Chen, Li-free cathode materials for high energy density lithium batteries, Joule 3 (2019) 2086–2102.
[2] Y. Lu, X. Rong, Y. Hu, L. Chen, H. Li, Research and development of advanced battery materials in China, Energy Storage Mater. 23 (2019) 144–153.
[3] N Watanabe, M Fukuda, Primary Cell for Electric Batteries, US Patent 3536532, (1970).
[4] G. Eichinger, J. Besenhard, High energy density lithium cells: Part II. Cathodes and complete cells, J. Electroanal. Chem. Interfacial Electrochem. 72 (1976) 1–31.
[5] Y. Shao, H. Yue, R. Qiao, J. Hu, G. Zhong, S. Wu, M.J. McDonald, Z. Gong, Z. Zhu, W. Yang, Y. Yang, Synthesis and reaction mechanism of novel fluorinated carbon fiber as a high-voltage cathode material for rechargeable Na batteries, Chem. Mater. 28 (2016) 1026–1033.
[6] P. Lam, R. Yazami, Physical characteristics and rate performance of (CFx)n (0.33< x< 0.66) in lithium batteries, J. Power Sources 153 (2006) 354–359.
[7] G. Nagasubramanian, M. Rodriguez, Performance enhancement at low temperatures and in situ X-ray analyses of discharge reaction of Li/(CFx)n cells, J. Power Sources 170 (2007) 179–184.
[8] F. Rao, Z. Wang, B. Xu, L. Chen, C. Ouyang, First-principles study of lithium and sodium atoms intercalation in fluorinated graphite, Engineering 1 (2015) 243–246.
[9] Y. Li, Y. Chen, W. Feng, F. Ding, X. Liu, The improved discharge performance of Li/CFx batteries by using multi-walled carbon nanotubes as conductive additive, J. Power Sources 196 (2011) 2246–2250.
[10] C. Peng, Y. Li, F. Yao, H. Fu, R. Zhou, Y. Feng, W. Feng, Ultrahigh-energy-density fluorinated calcinated macadamia nut shell cathodes for lithium/fluorinated carbon batteries, Carbon 153 (2019) 783–791.
[11] M.A. Reddy, B. Breitung, M. Fichtner, Improving the energy density and power density of CFx by mechanical milling: a primary lithium battery electrode, ACS Appl. Mater. Interfaces 5 (2013) 11207–11211.
[12] H. Groult, C. Julien, A. Bahloul, S. Leclerc, E. Briot, A. Mauger, Improvements of the electrochemical features of graphite fluorides in primary lithium battery by electrodeposition of polypyrrole, Electrochem. Commun. 13 (2011) 1074–1076.
[13] Y. Dai, S. Cai, L. Wu, W. Yang, J. Xie, W. Wen, J. Zheng, Y. Zhu, Surface modified CFx cathode material for ultrafast discharge and high energy density, J. Mater. Chem. 2 (2014) 20896–20901.
[14] Y. Li, W. Feng, The tunable electrochemical performances of carbon fluorides/manganese dioxide hybrid cathodes by their arrangements, J. Power Sources 274 (2015) 1292–1299.
[15] A. Lewandowski, P. Jakobczyk, Kinetics of Na|CFx and Li|CFx systems, J. Solid State Electrochem. 20 (2016) 3367–3373.
[16] E. Rangasamy, J. Li, G. Sahu, N. Dudney, C. Liang, Pushing the theoretical limit of Li-CFx batteries: a tale of bifunctional electrolyte, J. Am. Chem. Soc. 136 (2014) 6874–6877.
[17] J. Read, E. Collins, B. Piekarski, S. Zhang, LiF formation and cathode swelling in the Li/CFx battery, J. Electrochem. Soc. 158 (2011) A504–A510.
[18] K. Guérin, R. Yazami, A. Hamwi, Hybrid-type graphite fluoride as cathode material in primary lithium batteries, Electrochem. Solid St. 7 (2004) A159–A162.
[19] K. Kubota, M. Dahbi, T. Hosaka, S. Kumakura, S. Komaba, Towards K-ion and Na-ion batteries as "beyond Li-ion, Chem. Rec. 18 (2018) 459–479.
[20] A. Eftekhari, Z. Jian, X. Ji, Potassium secondary batteries, ACS Appl. Mater. Interfaces 9 (2017) 4404–4419.
[21] X. Bie, K. Kubota, T. Hosaka, K. Chihara, S. Komaba, A novel K-ion battery: hexacyanoferrate (II)/graphite cell, J. Mater. Chem. 5 (2017) 4325–4330.
[22] Y. Matsuda, H. Nakashima, M. Morita, Y. Takasu, Behavior of some ions in mixed organic electrolytes of high energy density batteries, J. Electrochem. Soc. 128 (1981) 2552–2556.
[23] G. Kresse, J. Furthmüller, Efficiency of ab-initio total energy calculations for metals and semiconductors using a plane-wave basis set, Comput. Mater. Sci. 6 (1996) 15–50.
[24] G. Kresse, J. Furthmüller, Efficient iterative schemes for ab initio total-energy calculations using a plane-wave basis set, Phys. Rev. B 54 (1996) 11169–11186.
[25] G. Kresse, D. Joubert, From ultrasoft pseudopotentials to the projector augmented-wave method, Phys. Rev. B 59 (1999) 1758–1775.
[26] J.P. Perdew, K. Burke, M. Ernzerhof, Generalized gradient approximation made simple, Phys. Rev. Lett. 77 (1996) 3865–3868.
[27] M.J. Frisch, G. Trucks, H. Schlegel, G. Scuseria, M. Robb, J. Cheeseman, G. Scalmani, V. Barone, B. Mennucci, G. Petersson, Gaussian 09, Revision D. 01, Gaussian, Inc., Wallingford, CT, 2009.
[28] A.D. Becke, A new mixing of Hartree–Fock and local density-functional theories, J. Chem. Phys. 98 (1993) 1372–1377.
[29] E. Cancès, B. Mennucci, J. Tomasi, A new integral equation formalism for the polarizable continuum model: theoretical background and applications to isotropic and anisotropic dielectrics, J. Chem. Phys. 107 (1997) 3032–3041.
[30] B. Mennucci, Polarizable continuum model, Wires. Comput. Mol. Sci. 2 (2012) 386–404.
[31] H. Touhara, K. Kadono, Y. Fujii, N. Watanabe, On the structure of graphite fluoride, Z. Anorg. Allg. Chem. 544 (1987) 7–20.
[32] L. Wang, J. Yang, J. Li, T. Chen, S. Chen, Z. Wu, J. Qiu, B. Wang, P. Gao, X. Niu, Graphite as a potassium ion battery anode in carbonate-based electrolyte and ether-based electrolyte, J. Power Sources 409 (2019) 24–30.
[33] W. Liu, H. Li, J. Xie, Z. Fu, Rechargeable room-temperature CFx-sodium battery, ACS Appl. Mater. Interfaces 6 (2014) 2209–2212.
[34] K. Zhong, X. Xia, B. Zhang, H. Li, Z. Wang, L. Chen, MnO powder as anode active materials for lithium ion batteries, J. Power Sources 195 (2010) 3300–3308.
[35] G. Yoon, H. Kim, I. Park, K. Kang, Conditions for reversible Na intercalation in graphite: theoretical studies on the interplay among guest Ions, solvent, and graphite host, Adv. Energy Mater. 7 (2017) 1601519.
[36] V. Gupta, T. Nakajima, Y. Ohzawa, B. Zemva, A study on the formation mechanism of graphite fluorides by Raman spectroscopy, J. Fluor. Chem. 120 (2003) 143–150.
[37] L. Wang, J. Zou, S. Chen, G. Zhou, J. Bai, P. Gao, Y. Wang, X. Yu, J. Li, Y.-S. Hu, TiS_2 as a high performance potassium ion battery cathode in ether-based electrolyte, Energy Storage Mater. 12 (2018) 216–222.
[38] K. Kubota, M. Dahbi, T. Hosaka, S. Kumakura, S. Komaba, Towards K-ion and Na-ion batteries as "beyond Li-ion", Chem. Rec. 18 (2018) 459–479.
[39] X. Niu, L. Li, J. Qiu, J. Yang, J. Huang, Z. Wu, J. Zou, C. Jiang, J. Gao, L. Wang, Salt-concentrated electrolytes for graphite anode in potassium ion battery, Solid State Ionics 341 (2019) 115050.
[40] N.T. Thanh, N. Maclean, S. Mahiddine, Mechanisms of nucleation and growth of nanoparticles in solution, Chem. Rev. 114 (2014) 7610–7630.
[41] Y. Tominaga, K. Yamazaki, V. Nanthana, Effect of anions on lithium ion conduction in poly(ethylene carbonate)-based polymer electrolytes, J. Electrochem. Soc. 162 (2015) A3133–A3136.

Cheng Jiang is currently pursuing his M.S. degree under the supervision of associate professor Liping Wang in University of Electronic Science and Technology of China. His current research interests focus on fluorinated carbons as high energy density cathodes.

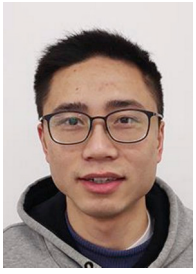

Bojun Wang is currently pursuing his Ph.D. under the supervision of Prof. Xiaobin Niu in the School of materials and Energy at the University of Electronic Science and Technology of China, China. He received his B.S. in electronic science and technology (2017) at University of Electronic Science and Technology of China, China. His current research interests focus on the growth mechanism of thin film and low dimensional materials.

Zhenrui Wu is currently a master's student at the University of British Columbia, Canada. His research investigates the ionic storage mechanism of carbon materials with different morphology and develops the electrochemical performance of carbon as anode or porous scaffold in both Li-ion batteries and K-ion batteries. He is also interested in the effects of electrolyte and its additive on ionic diffusion and ionic storage of carbon materials.

Jiliang Qiu received his bachelor degree from the University of Electronic Science and Technology of China (UESTC) in 2015. And now he is a PhD student following Prof. Liquan Chen and Prof. Hong Li in Institute of Physics, Chinese Academy of Sciences (IOP-CAS). His research interests focus on contrasting high energy density and safety solid-state battery, and the failure analysis of solid-state battery.

Zhengping Ding received his Bachelor's degree (2012) and Ph. D. degree in Materials Science (2017) from Central South University. Then, he worked as a R&D engineer at Tianjin Lishen Battery Joint-Stock Co., Ltd (2018). He is now working as a "Boya" postdoctoral research fellow in Electron Microscopy Laboratory at Peking University. He was awarded excellent postdoctoral thesis of Central South University. His main research interests focus on the synthesis and application of nanomaterials for clean energy storage, the relationship between structure and electrochemical properties and in-situ transmission electron microscopy in energy storage materials.

Jian Zou received his master's degree in University of Electronic Science and Technology of China (UESTC) in 2018. He is currently a Ph.D. candidate at School of Materials and Energy in UESTC. His main research interests focus on the development of high energy density cathodes for Li ion batteries.

Shulin Chen is currently a Ph.D. candidate in School of Materials Science, Harbin Institute of Technology. He received his Bachelor's degree from Harbin Institute of Technology in 2015. He joined Prof. Peng Gao's group in February 2016 as a joint Ph.D. candidate. His research interests are in situ TEM for lithiation or sodiation of TMD and probing the structure and decomposition mechanism of $MAPbX_3$.

Peng Gao is an assistant Professor in School of Physics, Peking University, Beijing, China. He received his Ph.D. degree in condensed mater physics from the Institute of Physics, Chinese Academy of Sciences in 2010. He was a postdoctor in University of Michigan (2010–2013), research associate in Brookhaven National Lab (2013–2014), research fellow and Japan Society for the Promotion of Science (JSPS) foreign fellow in University of Tokyo (2014–2015). He joined in Peking University in 2015. His research interests include electron microscopy, ferroelectrics, solid-state ionics, and structure and properties of crystal defects and interfaces.

Xiaobin Niu is now a Professor at University of Electronic Science and Technology of China (UESTC). He received his B.S. in Physics (2000) and M.S. in Physics (2003) at University of Science and Technology of China (USTC), China. He received his Ph.D. degree in Materials Science and Engineering from University of California, Los Angeles in 2008. His research interest lies in the modelling and simulation of materials from the atomic to mesoscopic scales.

Liping Wang is an associate professor in University of Electronic Science and Technology of China. She received her PhD degree (2011) in Institute of Physics, Chinese Academy of Sciences and Laboratoire de réactivité et chimie des solides (LRCS), Université de Picardie Jules Verne, France. She worked as a post-doctoral fellow in Max Planck Institute of Colloids and Interfaces, Germany (2012) and Research Associate at Brookhaven National Lab, United States (2013–2014). Her current research interests are high energy density Li batteries.

Hong Li got the bachelor degree in Lanzhou University in 1992, master degree in CAS in 1995, and Ph.D degree in Institute of Physics, CAS in 1999. He is currently a full professor in Institute of Physics, Chinese Academy of Sciences. His research interest is high energy density lithium ion batteries, solid lithium batteries and failure analysis. He is the regional editor of Solid State Ionics and Ionics. He has initiated the Tianmu-lake Institute of Advanced Energy Storage, Yangtze River Delta Physics Research Center, Beijing WeLion New Energy Tech. Ltd., Tianmu Excellent Anode Materials Tech. Ltd, HiNa Battery Tech. Ltd.